Microtearing Mode Fluctuations in Reversed Field Pinch Plasmas

D. Carmody[1], P.W. Terry[1], M.J. Pueschel[1], J.S. Sarff[2] and Y. Ren[2]

[1]Department of Physics, University of Wisconsin - Madison, Madison, Wisconsin 53706
[2]Princeton Plasma Physics Laboratory, Princeton, New Jersey

Corresponding Author: dcarmody@wisc.edu

Abstract:

Improved confinement scenarios in RFP plasmas that reduce global tearing modes are expected to lead to plasmas where confinement is limited by microturbulence driven by gradients of pressure, density, and temperature. Because enhanced confinement regimes in MST yield temperature profiles with core gradients near the critical threshold for temperature-gradient driven instability, a linear analysis of temperature-gradient driven micro-instabilities in MST-like RFP equilibria is undertaken using toroidal gyrokinetics for beta values ranging from 0 to 10%. These simulations show that when a/L_T is greater than $3-4$, MST plasmas are unstable to ITG at low beta and unstable to microtearing at high beta. The beta at which microtearing dominates ITG is 5%, with ITG becoming completely stable just above 10%. Theory shows that the higher critical beta for ITG stabilization, relative to tokamaks, is associated with the shorter scale lengths for magnetic curvature. At the MST-relevant beta of 9% the microtearing mode growth rate peaks at a poloidal wavenumber of $k_\theta = 1.5$ inverse gyroradii. However, instability is strong even for low wavenumbers, where there is a growth rate $2-3$ times that of ITG at its maximal wavenumber for zero beta. The growth rate remains large even for very low collisionality, with indications that different microtearing branches are associated with low and moderate collisionalities. With these growth rate values significant transport is expected. MST has several diagnostics that will access microturbulence spatial scales, including FIR interferometry/scattering, fast Thomson scattering, heavy ion beam probe, and material probes. Work is underway to prepare these diagnostics for electrostatic and magnetic turbulence measurements for model validation in high-performance plasmas.

1 Introduction

Improved confinement scenarios in reversed field pinch (RFP) plasmas that reduce global tearing mode activity are expected to lead to plasmas, like in tokamaks, where confinement is limited by pressure, density, and temperature gradient driven microturbulence. Indeed, measurements in MST and RFX-Mod yield temperature profiles with gradients in the core that are near the critical threshold for temperature gradient driven microtearing and/or ion temperature gradient (ITG) instability. Steep gradient conditions are arrived at using current profile control to reduce tearing instability, or spontaneously through

a self-organized transition to quasi-single-helicity (QSH) states. This type of situation is complemented by correlation analysis of high frequency magnetic turbulence. While this turbulence appears to be part of the cascade from unstable tearing modes, it has a standing wave structure that is consistent with microtearing modes or collisionless shear Alfven modes, but little else [1]. To model these types of plasmas and begin assembling the capability for validation we undertake linear analysis of temperature gradient driven micro-instabilities in MST-like RFP equilibria using toroidal gyrokinetics for beta values ranging from 0 to 10%. These simulations show that the microtearing mode is unstable in steep gradient MST plasmas where $\beta \sim 10\%$ and is capable of producing significant transport.

2 Finite Beta Gyrokinetic Simulations

To have readily available RFP equilibria for toroidal gyrokinetic solvers, a model equilibrium has been derived from the Grad-Shafranov equation. This equilibrium, the toroidal Bessel function model (TBFM), is implemented in the gyrokinetic code GYRO [2] and has the following form,

$$B_\phi = \frac{B_0}{R} J_0(2\Theta r/a), \quad B_\theta = \frac{B_0}{R} J_1(2\Theta r/a) \tag{1}$$

where a is the minor radius, $R = R_0(1 + (r/R_0)cos\theta)$, and Θ is the RFP pinch parameter, defined by $\Theta = \langle B_\theta \rangle^{wall} / \langle B_\phi \rangle^{vol}$. This equilibrium has been benchmarked with the $s - \alpha$ model for RFP parameters, which does not give very accurate growth rates, and with the Miller equilibrium, which gives good growth rates except at large r.

Using the TBFM, a series of electrostatic simulations are performed, and in this zero beta limit it is found that the dominant gyroscale instability is ITG. This is marked by a ballooning parity in the eigenmode structure (even in ϕ and odd in $A_\parallel$) and a frequency in the ion diamagnetic direction. Drawing off the ion temperature gradient as its free energy source, this instability is found to require a threshold gradient of $a/L_{T_i} > 3 - 4$ to become unstable in MST-like discharges.

Finite beta simulations reveal a beta suppression of the ITG mode and a transition of the dominant instability from ITG to a microtearing mode, with microtearing becoming dominant in the growth rate spectrum for $\beta > 5\%$ (Figure 1). Finite beta stabilization of ITG occurs as in the tokamak, through coupling to shear Alfven waves, and is controlled by the parameter $d\beta/dr$. An analysis of beta suppression of ITG in a tokamak equilibrium has been done by Hirose [6]. Adjusting this analysis for the RFP equilibrium, it is found that the critical β for stabilization is higher than the tokamak β by a factor proportional to the aspect ratio, a consequence of the smaller scale length for magnetic curvature in the RFP equilibrium where $B_\theta \approx B_\phi$. The condition for stability of ITG is found to be

$$\beta_e \geq \frac{\varepsilon_n \epsilon^2 \tau^2}{(1 + (\epsilon/q)^2) q^2 [(\tau + 2\varepsilon_n)(\tau + 1) + \tau^2 \eta_e]} \tag{2}$$

Choosing parameters similar to those used for the growth rates plotted in Fig. 1 ($\tau = T_e/T_i = 2.5, \varepsilon_n = a/L_n = 1/.58, \eta_e = L_{n_i}/L_{T_i} = 8.6, q = 1/5, \epsilon = 1/3$), the above

expression yields a critical beta of approximately 10.6%. This behavior can be seen in Fig. 1, where the dominant instability is plotted across a range of beta for two different values of the electron temperature gradient, above and below the threshold for microtearing. For $a/L_{Te} = 3.0$, the microtearing mode is stable, and the beta suppression of ITG can clearly be seen, with a critical beta occuring at roughly 10%.

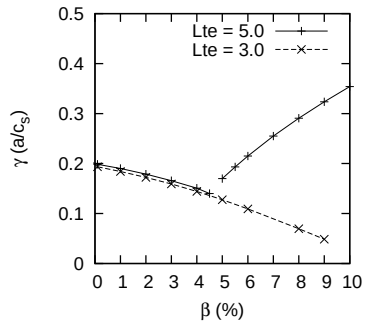

FIG. 1: Beta dependence and mode transition. Shown is the growth rate for a mode at $k_\theta \rho_s = 0.365$. The dashed line shows $a/L_{T_e} = 3.0$, where microtearing is stabilized and the beta suppression of ITG can be seen.

The mode that becomes the dominant instability above $\beta \sim 5\%$ has mode structure along the magnetic field line with odd parity in the electrostatic potential and even parity in the vector potential. This, and a mode frequency in the electron direction, identify the mode as microtearing. The kinetic ballooning mode is not seen for these parameters. Like recent reports of unstable microtearing in the RFP [3] and for standard and spherical tokamak geometries [4,5], the potential mode structure is very extended in ballooning space (Figure 2). The mode has a temperature gradient threshold that is very close to that of ITG, requiring $a/L_{T_e} > 3 - 4$ for instability, but with a much steeper rise in growth rate with increased temperature gradient. This is shown in Fig. 3 a). The peak of the growth rate spectrum increases as β increases. Near the critical β the spectrum peaks at low k_y as in ITG. At the MST-relevant $\beta = 9\%$ the growth rate is maximum at $k_y \rho_s = 1.4$. However, even at $k_y \rho_s = 0.5$ the microtearing growth rate for $\beta = 9\%$ is a factor of $2 - 3$ larger than the maximal ITG growth rate at this wavenumber for $\beta = 1\%$. This behavior is shown in Fig. 3 b).

With a large growth rate even at low k_y it is expected that microtearing will yield significant electron thermal transport. The steep rise of growth with temperature gradient will produce profile stiffness in the temperature gradient.

2.1 Collisions

Collisions are thought to play an important role in the mechanisms that drive the microtearing instability. This includes physics due to the time-dependent thermal force [7-9] and contributions from trapped particles [10]. The variation of the growth rate with collisionality can be seen in Figure 4. Stable at high collisionality, the growth rate achieves a

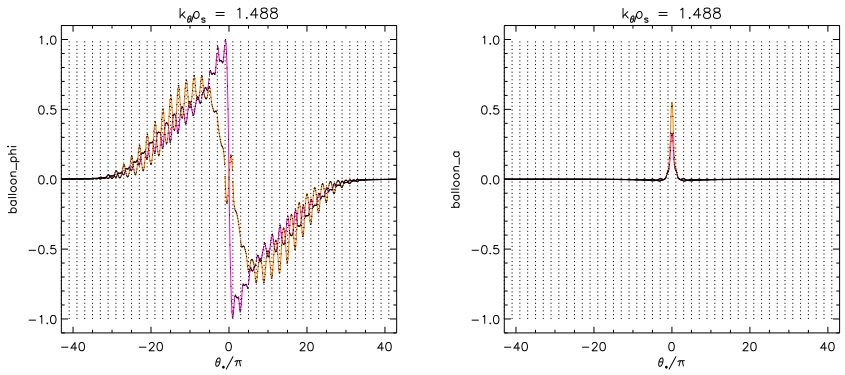

FIG. 2: Microtearing eigenmode structure - electrostaic potential (left) and magnetic vector potential (right).

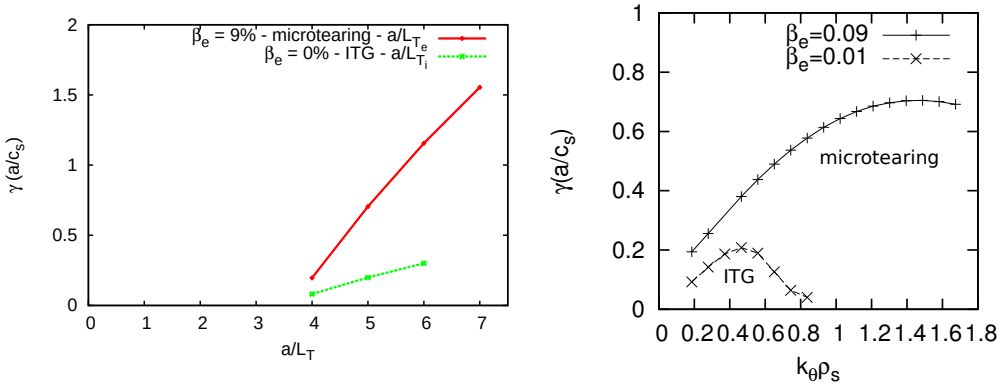

FIG. 3: a) Growth rate as a function of temperature gradient scale length for ITG at zero β (solid line) and microtearing at $\beta = 9\%$ (broken line). b) Growth rate spectra in k_y for ITG at zero β and microtearing at $\beta = 9\%$.

peak near $\nu \sim 1$, which lies in the semi-collisional range [9]. Surprisingly, the growth rate remains significant even in the collisionless limit. The mechanism for this is unclear, since collisions are believed to be necessary for instability. A possible mechanism might arise due to the presence of a strong curvature drift. A drift-tearing mode requiring both an electron temperature gradient and curvature drift has been found to exist for the RFP in the semi-collisional range [11], but as of yet no theory exists for the collisionless regime. The effects of varying the strength of the curvature drift in the gyrokinetic simulations can be seen in Figure 5. Here the growth rate of the microtearing instability is plotted against a factor α multiplying the curvature drift. The true physical drift is given by $\alpha = 1$. It can be seen that the mode is stabilized for curvature drifts less or greater than the physical value. Results for both $\nu = 1.0$ and $\nu = 0.001$ are given, showing that likely the same mechanism underlies the instability in both the collisionless and semi-collisional regimes. Varying the RFP pinch parameter Θ (Figure 6) reveals that there are different responses in the collisionality scan at low and moderate collisionality. This suggests that

there are possibly different mechanisms for the instability in these two regimes and they represent different microtearing branches.

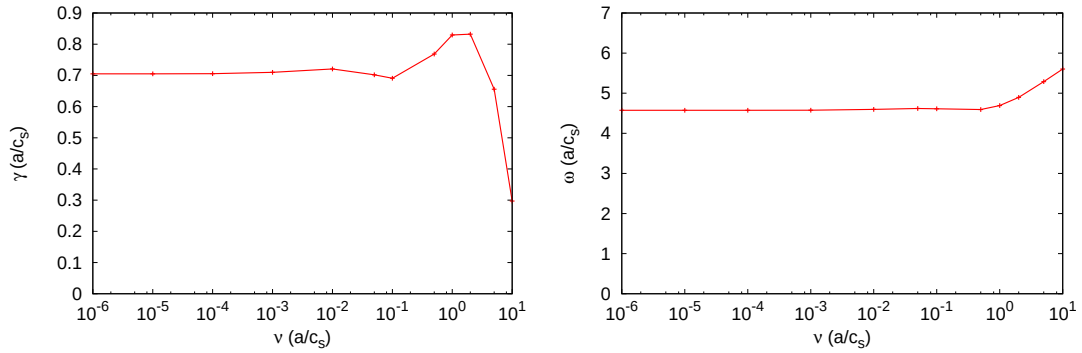

FIG. 4: Scan over collisional frequency for $\beta = 9\%$ and $k_\theta \rho_s = 1.488$, growth rate (left) and frequency (right).

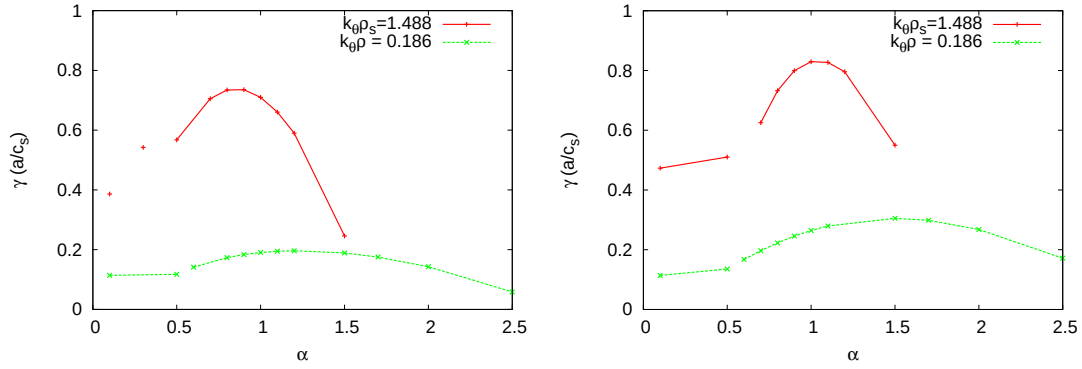

FIG. 5: The role of curvature drift in the RFP microtearing instability. The α parameter is a factor multiplying the curvature drift. The left figure is for $\nu = 0.001$ and the right figure is for $\nu = 1.0$. The two points in each plot at the lowest values of α are not microtearing and have not been identified.

3 Experimental Perspective

The MST facility has several diagnostics that will access microturbulence spatial scales ($k_\perp \rho_i < 1$), including FIR interferometry/scattering, fast Thomson scattering, heavy ion beam probe, and material probes. Work is underway to prepare these diagnostics for electrostatic and magnetic turbulence measurements in high-performance plasmas attained with pulsed parallel current drive (PPCD) and/or QSH transitions. The possibility of comparing predictions of the gyrokinetic model for RFP microturbulence with data from

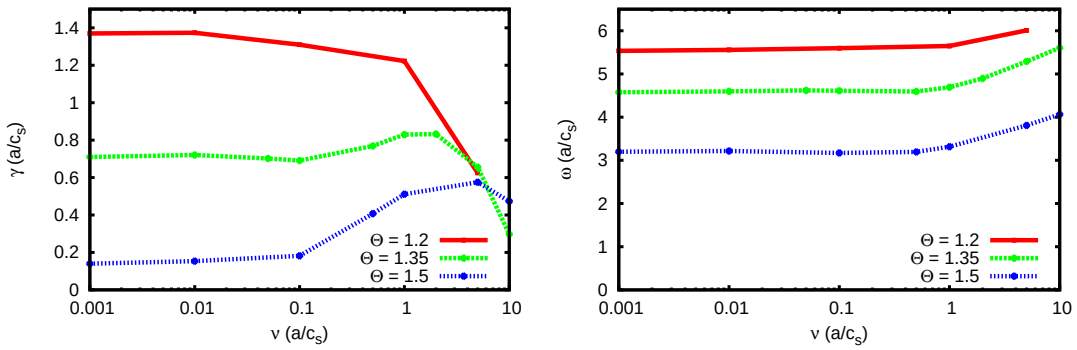

FIG. 6: The effect on collisional scaling by varying the RFP pinch parameter, Θ.

as many as four independent fluctuation diagnostics is very appealing from the standpoint of validation and quite unique. There is also the opportunity for experimental comparisons with standard RFP plasmas, which have relatively flat pressure profiles in the core, and are likely linearly stable to drift-wave-like instabilities. Microturbulence might nevertheless appear as a consequence of a turbulent cascade driven by unstable tearing modes. Recent measurements of broadband magnetic turbulence in MST standard RFP plasmas reveal wavenumber power spectra with scaling features well described by a dissipative nonlinear cascade [1]. For example, as the fluctuation power in the long-wavelength tearing modes rises or falls, the power in shorter wavelengths follows in concert as a featureless spectrum that extends to the ion gyroradius scale. Correlation measurements reveal a radial standing wave structure for the shorter wavelength portion of this spectrum that could be explained by nonlinearly excited microtearing or collisionless shear Alfven modes. Other candidates for small scale RFP instability, such as resistive interchange and current driven drift waves, do not have the standing wave feature. These measurements will be presented as a possible means to explore drift-wave-like modes when the pressure profile has sub-critical gradients.

4 Conclusion

This research used a model RFP equilibrium, the toroidal Bessel function model, and the gyrokinetic code GYRO to investigate the characteristics of gyroscale instabilities in the Madison Symmetric Torus. It was found that the dominant instability at low beta was ITG, yielding to a microtearing mode above a β of about 5%. Both ITG and microtearing require temperature gradient above a threshold of $a/L_T > 3-4$ for instability, with a much sharper rise in the microtearing growth rate with temperature gradient. This microtearing mode is driven by the electron temperature gradient and shows some dependence on collisionality, but maintains a strong positive growth rate even in the collisionless limit. Given the strength of the mode and the wide range of scales across which it is unstable, it is expected that microtearing will make large contributions to electron thermal transport

in the RFP. A suite of diagnostics employed on the Madison Symmetric Torus provide measurements of electrostatic and magnetic turbulence.

Work supported by USDOE Grant No. DE-FG-02-85ER53212

References

[1] REN, Y. et al., Phys. Rev. Lett. 107 (2011) 195002.

[2] TANGRI, V., TERRY, P.W., and WALTZ, R.E., Phys. Plasmas 18 (2011) 052310.

[3] PREDEBON, I., et al., Phys. Rev. Lett. 105 (2010) 195001.

[4] DOERK, H., et al., Phys. Rev. Lett. 106 (2011) 155003.

[5] GUTTENFELDER, W., et al., Phys. Rev. Lett. 106 (2011) 155004.

[6] HIROSE, A., Physics of Plasmas 7 (2000) 433436.

[7] HAZELTINE, R.D., DOBROTT, D., and WANG, T.S., Physics of Fluids 18 (1975) 1778.

[8] GLADD, N.T., DRAKE, J.F., CHANG, C.L., and LIU, C.S., Physics of Fluids 23 (1980) 1182.

[9] DRAKE, J.F. and LEE, Y.C., Physics of Fluids 20 (1977) 1341.

[10] CATTO, P.J. and ROSENBLUTH, M., Physics of Fluids 24 (1981) 243.

[11] FINN, J.M., and DRAKE, J.F., Physics of Fluids 29 (1986) 3672.